MOLECULAR AND CELLULAR BIOLOGY, June 1988, p. 2379–2393
0270-7306/88/062379-15$02.00/0

Vol. 8, No. 6

RNA11 Protein Is Associated with the Yeast Spliceosome and Is Localized in the Periphery of the Cell Nucleus

TIEN-HSIEN CHANG, MICHAEL W. CLARK, ARTHUR J. LUSTIG,† MICHAEL E. CUSICK, AND JOHN ABELSON*

Division of Biology, California Institute of Technology, Pasadena, California 91125

Received 7 January 1988/Accepted 9 March 1988

The yeast *rna* mutations (*rna2* through *rna10/11*) are a set of temperature-sensitive mutations that result in the accumulation of pre-mRNAs at the nonpermissive temperature. Most of the yeast *RNA* gene products are involved in and essential for mRNA splicing in vitro, suggesting that they code for components of the splicing machinery. We tested this proposal by using an in vitro-synthesized RNA11 protein to complement the temperature-sensitive defect of the *rna11* extract. During the in vitro complementation, the input RNA11 protein was associated with the 40S spliceosome and a 30S complex, suggesting that the RNA11 protein is indeed a component of the spliceosome. The formation of the RNA11-associated 30S complex did not require any exogenous RNA substrate, suggesting that this 30S particle is likely to be a preassembled complex involved in splicing. The RNA11-specific antibody inhibited the mRNA splicing in vitro, confirming the essential role of the RNA11 protein in mRNA splicing. Finally, using the anti-RNA11 antibody, we localized the RNA11 protein to the periphery of the yeast nucleus.

Through the development of in vitro splicing systems, a two-step biochemical pathway for the removal of introns from nuclear mRNA precursors (pre-mRNAs), referred to as mRNA splicing, has been delineated (for a review, see reference 42). This splicing reaction is done on a 40S to 60S macromolecular complex, the spliceosome, on which the reaction intermediates are confined (4, 15, 16). It is becoming apparent that the complexity of such a large particle may well be as great as that of the ribosomal subunits and that it could contain a number of proteins and several RNAs.

To date, five major classes of small nuclear RNAs (snRNAs; U1, U2, U4 to U6) have been found to be involved in mammalian mRNA splicing (for a recent review, see reference 37). Of these, four (U1, U2, U4, and U5) possess a 5′ trimethylguanosine (m_3G) cap. All five snRNAs are tightly associated with one or more proteins and function in the form of small nuclear ribonucleoprotein particles (snRNPs) (48, 56). The human autoimmune antiserum anti-Sm has been used to precipitate these snRNAs and to demonstrate that these snRNAs are required for mRNA splicing (28, 43). The Sm antigens are a subset of snRNP proteins found in all five of the snRNPs which function in mRNA splicing (48). In yeasts, snRNAs also possess the 5′ m_3G cap structure which renders them immunoprecipitable by the anti-m_3G antibody (reviewed in reference 18). Furthermore, a subset of yeast snRNAs (e.g., snR7, snR14, and snR20) contain potential Sm antigen-binding sites in their single-stranded regions with a consensus sequence of $A(U_{3-6})G$ (2, 19, 44, 49, 50, 60). Indeed, some of the human anti-Sm antisera can precipitate these snRNAs from the yeast extract (50, 60; S.-C. Cheng and J. Abelson, unpublished data).

Recent analyses of the spliceosomal components performed either by affinity purification of the spliceosome or by native gel fractionation of the in vitro splicing systems have revealed that several snRNPs (U2, U5, and U4 + U6 for mammalian cell systems; snR6, snR7, snR14, and snR20 for the yeast system) reside on the spliceosomes (8, 17, 26, 27, 46, 47). In addition, the involvement of the heterogeneous nuclear RNP (hnRNP) complexes in mRNA splicing and spliceosome formation has been implicated by inhibition experiments with antibodies against the hnRNP core proteins (9, 53). Spliceosome assembly follows a rather complicated pathway, with several spliceosome intermediates appearing in sequence (8, 17, 27, 46, 47). The apparent complexity of the spliceosome and the mRNA splicing process demands a combined effort by both biochemical fractionation and genetic analysis to enumerate all the components involved in mRNA splicing and eventually to understand their functions.

Taking advantage of the well-characterized genetic properties and the readily available mutants of the yeast *Saccharomyces cerevisiae*, we have begun to analyze the mRNA-splicing mechanism in detail. In particular, special attention has been focused on a set of temperature-sensitive mutations initially isolated by Hartwell (20) which form nine complementation groups denoted *rna2* to *rna10/11* (36). Although originally thought to be defective in general RNA metabolism, these *rna* mutants turn out to be functionally impaired in mRNA splicing at the nonpermissive temperature in a very specific manner (51; reviewed in reference 36). By developing an in vitro complementation assay, Lustig et al. (36) have shown that many of the *RNA* genes are likely to code for products directly involved in and essential for mRNA splicing. In addition, most of the *RNA* gene products are required for the formation of spliceosomes in vitro, with an exception of the *RNA2* gene product, which is a factor extrinsic to the spliceosome (33). On the basis of these studies, Lin et al. (33) proposed a three-step mechanism for mRNA splicing and deduced multiple intrinsic and extrinsic factors which are involved in the formation of the spliceosome.

We proceeded to examine the role of one of the *RNA* gene products, the RNA11 protein, in mRNA splicing and its relationship to the spliceosome. In this study, we first demonstrated that the in vitro-synthesized RNA11 protein is

* Corresponding author.
† Present address: Program in Molecular Biology, Memorial Sloan-Kettering Cancer Center, New York, NY 10021.

capable of complementing the defects of heat-sensitive *rna11* extracts. We then provided evidence that the RNA11 protein is specifically associated with the 40S spliceosome and with a 30S complex. Finally, using an anti-RNA11 antibody, we showed that the RNA11 protein is essential for mRNA splicing in vitro and is localized predominantly in the periphery of the yeast nucleus.

MATERIALS AND METHODS

Yeast strains. The following yeast strains were used in this study: the wild-type strain EJ101; *rna2* strain SS304; *rna5* strain RL173; *rna11* strains SPJ11.4 and AJL145.9d. The genotypes of these strains have been described by Lin et al. (34) and Lustig et al. (36).

Isolation of yeast splicing extracts. Extracts were prepared from cells grown to the mid- to late log phase at 23°C in YPD medium as described by Lustig et al. (36).

Preparation of splicing substrates. The wild-type and C259 actin transcripts used in this study have been described previously (34, 58). Low-specific-activity transcripts and antisense transcript were synthesized by the methods of Cheng and Abelson (8).

Plasmid constructions and oligonucleotide-directed site-specific mutagenesis. Plasmid pAS1 containing the wild-type *RNA11* gene in a 4.6-kilobase (kb) *Hin*dIII fragment cloned into pBR322 was kindly provided by R. Sternglanz of the State University of New York at Stony Brook. Plasmid M13mp10-*RNA11* was constructed by subcloning a 2.7-kb *Bam*HI-*Hin*dIII fragment encompassing the entire *RNA11* gene into M13mp10. Two oligonucleotides with the following sequences were synthesized and utilized to introduce a *Pst*I or *Eco*RI site just upstream of the *RNA11* gene: 5′-CCCTTCTTACCTGCAGCTATTTGTGA-3′ (26mer/*Pst*I) and 5′-TTTGAATTCTTGGATGCGTTA-3′ (21mer/*Eco*RI). Oligonucleotide mutagenesis was performed as described by Newman et al. (40). After the mutagenesis, *RNA11*-containing DNA fragments *Pst*I-*Xba*I and *Eco*RI-*Hin*dIII were transferred to pSP64 (39) and pKK223-3 (5) vectors, respectively. Plasmids pSP64-*RNA11* and pKK223-3-*RNA11* were then used to transform *Escherichia coli* strains MC1061 [F^- *araD139* Δ(*araABIOC-leu*)*7679* Δ(*lac*)*x74 galU galK rpsL hsr hsm*$^+$] and JM105 [Δ(*lac-pro*) *thi strA endA sbcB15 hspR4 F′ traD36 proAB lac*I^{q}ZΔM15), respectively.

In vitro transcription and in vitro translation. In vitro transcription was performed essentially as described by Melton et al. (39). The DNA templates used in the runoff transcription reactions were generated by *Eco*RI or *Hae*III linearization of the pSP64-*RNA11* plasmid. Linear DNA templates (50 μg/ml) were transcribed in 50 mM Tris (pH 7.5)–6 mM $MgCl_2$–20 mM NaCl–1 mM spermidine–10 mM dithiothreitol–RNasin (1 unit/μl)–0.5 mM each ribonucleoside triphosphate. Typically, 20 U of SP6 polymerase (Promega Biotec, Madison, Wis.) per μg of DNA template was added for 2 to 3 h of synthesis at 37°C. After RNA synthesis, the reactions were terminated by phenol-chloroform extraction and then precipitated directly by the addition of Tris (pH 8.0) to 0.5 M and 2 volumes of ethanol. The ethanol precipitation was repeated three times to remove residual contaminants. To monitor the RNA synthesis, we assembled a small-scale reaction mixture supplemented with 5 μCi of [α-^{32}P]UTP (3,000 Ci/mmol; Amersham Corp., Arlington Heights, Ill.), and the RNA molecules synthesized were analyzed by 6% denaturing gel (19:1, acrylamide-bisacrylamide) electrophoresis and autoradiography.

To synthesize ^{35}S-labeled proteins in vitro, we used the rabbit reticulocyte lysate system (New England Nuclear Corp., Boston, Mass.) and L-[^{35}S]methionine (1,380 Ci/mmol; Amersham). In vitro translation reactions were performed following the instructions provided by New England Nuclear Corp. In a typical 25-μl reaction mixture, 1.5 μg of *RNA11* transcript or globin transcript (Bethesda Research Laboratories, Inc., Gaithersburg, Md.) was incubated together with 10 μl of rabbit reticulocyte lysate, 5.5 μl of translation cocktail, 2 μl of 1 M potassium acetate, 0.5 μl of 32.5 mM magnesium acetate, and 30 μCi of L-[^{35}S]methionine at 37°C for 1 h. Translated proteins were analyzed by removing 1-μl samples from each reaction mixture and fractionating them by sodium dodecyl sulfate-10% polyacrylamide gel electrophoresis (SDS-PAGE; 30). After electrophoresis, the gel was treated with 1 M sodium salicylate at room temperature for 30 min and dried under a vacuum. The dried gel was then subjected to autoradiography at −70°C with an intensifying screen. The translated proteins in the reaction mixture were used directly for in vitro complementation without further purification.

In vitro complementation and glycerol gradient analysis. The in vitro complementation procedure was developed based on that of Lustig et al. (36), in which heat inactivation and splicing were done successively. For heat inactivation, 7 μl of yeast extract was mixed with 2.2 μl of cocktail 1 (15 mM $MgCl_2$, 6.1 mM dithiothreitol, 16 units of RNasin) and 3 μl of translation mix (or an equivalent amount of water) and incubated at 32°C for 1 h. The reaction conditions were then adjusted for splicing by adding 1.7 μl of cocktail 2 (300 mM KPO_4 [pH 7.0], 20 mM ATP, 20% polyethylene glycol 8000) and 3.5 μl of ^{32}P-labeled transcript (20,000 cpm/μl). Splicing was done at 15°C for 30 min. For minus ATP reactions, the ATP in cocktail 2 was left out. For nonfunctional complementation, 7 μl of yeast extract was incubated with 2.2 μl of cocktail 3 (11.4 mM $MgCl_2$, 4.5 mM dithiothreitol, 12 units of RNasin) at 32°C for 1 h. Subsequently, the translation mix, cocktail 2, and ^{32}P-labeled transcript were added for splicing as described above for complementation reactions.

For gradient analysis, the complementation mixture was diluted with 25 μl of gradient buffer without glycerol (50 mM KCl, 2 mM $MgCl_2$, 20 mM HEPES-K^+ [potassium–*N*-2-hydroxyethylpiperazine-*N*′-2-ethanesulfonic acid] [pH 7.4]) and layered on a 11 to 23% glycerol gradient (4.4 ml in a 2-in. [5-cm] polyallomer centrifuge tube). The sedimentation was performed at 23,700 × *g* (50,000 rpm) for 90 min at 2°C in a Beckman SW55 rotor. Fractions were collected, and radioactivities were determined by Cerenkov counting. Proteins and nucleic acids in each fraction were then precipitated by the addition of Triton X-100 to 0.1% and trichloroacetic acid to 5% and chilled to −20°C overnight. The trichloroacetic acid precipitates were collected by centrifugation, neutralized by 2 μl of 2 M Tris (pH 9.0), and suspended in 15 μl of gel loading buffer (60 mM Tris [pH 6.8], 2% SDS, 10% glycerol, 40 mM β-mercaptoethanol, 0.02% bromophenol blue). The samples were then boiled for 3 min and loaded on an SDS-14% polyacrylamide gel (30) for electrophoresis. In some cases, as noted in the text, the complementation reaction mixture was treated with 2 μg of heparin for every microliter of yeast extract used in the reaction before gradient analysis.

Overproduction of RNA11 protein in *E. coli*. The RNA11 protein in an *E. coli* strain, JM105(pKK223-3-*RNA11*), was overproduced by isopropyl-β-D-thiogalactopyranoside (IPTG) induction as described by Phizicky et al. (45). At the end of IPTG induction, cells were harvested and lysed directly in protein gel loading buffer containing SDS and β-mercaptoethanol. Typically, 80 μl of Tris-sucrose buffer

(10 mM Tris [pH 7.4], 10% sucrose) was added for every milliliter of culture volume per unit of optical density at 550 nm to suspend cells. The 5× gel loading buffer (0.3 M Tris [pH 6.8], 10% SDS, 50% glycerol, 2 M β-mercaptoethanol, 0.1% bromophenol blue) was then added to a final concentration of 1×. Samples (10 to 15 μl) were boiled before being loaded on protein gels (30). A silver staining technique (62) was used to visualize the proteins on the gel.

Preparation of the anti-RNA11 antibody and immunoblot analysis. The overproduced RNA11 protein was first separated from the bulk protein in the *E. coli* crude lysate by ammonium sulfate precipitation (55% cut), loaded on a heparin-agarose column, and eluted with a linear salt gradient (0.1 to 1.5 M NaCl). The peak fractions containing the RNA11 protein (between 0.2 and 0.6 M NaCl) were pooled and concentrated by ammonium sulfate precipitation. Further purification of the RNA11 protein was achieved by SDS-14% PAGE (30), and gel slices which contained the RNA11 protein were then utilized to immunize New Zealand White male rabbits as described by Phizicky et al. (45). The antibody thus obtained was used in immunoblot analysis to detect RNA11 protein in yeast extract or crude lysate prepared from the RNA11-overproducing *E. coli* strain. The procedures of electroblotting proteins onto nitrocellulose filters and visualization of the RNA11 protein with anti-RNA11 antibody, biotinylated secondary antibody, and horseradish peroxidase have been described previously (10, 57).

Immunoprecipitation. Anti-m_3G cap antibody and anti-Sm (no. 58) human autoimmune antibody were generous gifts from R. Lührmann (Max-Planck-Institute, Berlin, Federal Republic of Germany) and S. Hoch (Agouron Institute, La Jolla, Calif.), respectively. The immunoprecipitation was performed essentially as described by Wolin and Steiz (61). Antibodies (from anti-Sm, anti-m_3G, and anti-RNA11 antisera or preimmune serum) were coupled to 2.5 mg of protein A-Sepharose (Pharmacia, Inc., Piscataway, N.J.) in 0.5 ml of NET-2 buffer (50 mM Tris [pH 7.4], 150 mM NaCl, 0.05% Nonidet P-40) at room temperature for 1 h. After NET-2 washes, the antibody-bound protein A-Sepharose was incubated with either in vitro translation reaction mixtures or in vitro complementation mixtures at 4°C for 1 h. The pellets were then washed extensively with NET-2 buffer and analyzed by protein gel electrophoresis followed by autoradiography. The ^{35}S radioactivity was determined by incubating the gel slices of interest in 10 ml of Econofluor containing 3% Protosol (New England Nuclear Corp.) overnight at 37°C and subsequent liquid scintillation counting.

Antibody inhibition of mRNA splicing in vitro. Wild-type yeast extract (7 μl) was mixed with 7 μl of protein A-purified antibody or with lesser amounts of antibody plus buffer D (20 mM HEPES (pH 7.9), 0.2 mM EDTA, 0.5 mM dithiothreitol, 50 mM NaCl, 20% glycerol) to a final volume of 7 μl and incubated together for 30 min at 0°C. Then a solution containing ^{32}P-labeled RNA transcript (20,000 cpm/μl) plus all other components necessary for splicing (33) was added to a final volume of 20 μl. The splicing reaction mixture was incubated at 23°C for 30 min. Reactions were stopped and analyzed by denaturing PAGE as previously described (33).

Immunofluorescence microscopy. Immunofluorescence microscopy was modified from the techniques for whole-mount yeast cells developed by Kilmartin and co-workers (1, 25). Because of the relatively low copy number of the RNA11 protein in the yeast cell, the cells were mounted for immunofluorescence by the postfixation procedure detailed by Clark and Abelson (10). The cells were converted into spheroplasts by enzymatic digestion, washed, and then mounted on the polylysine-coated slide and fixed with 3.7% formaldehyde in 0.1 M potassium phosphate-citrate (pH 6.5)–1.2 M sorbitol for 10 min. After fixation, the mounted, fixed spheroplasts were passed through −20°C methanol and acetone for 6 min and 30 s, respectively, and then air dried and stored at 6°C until used. These mounted spheroplasts were then stained for immunofluorescence by the application of 0.1 ml of a 1:500 dilution of the anti-RNA11 antiserum in 20 mM potassium phosphate (pH 7.0)–150 mM NaCl (phosphate-buffered saline)–0.1 mg of bovine serum albumin per ml directly to the spheroplasts and incubated at 6°C for 16 to 18 h. For the double-label experiment, the anti-RNA11 antiserum was added directly to the human autoimmune nucleolar (fibrillarin)-staining solution (ANA-N; Sigma Chemical Co., St. Louis, Mo.) at a 1:500 dilution. This solution was used in the same manner as described above. After the primary incubation, the slides were washed with buffer and incubated with a 1:100 dilution in phosphate-buffered saline-bovine serum albumin of anti-rabbit immunoglobulin G (IgG)-fluorescein isothiocyanate (Sigma) or, for the double-lable experiment, a 1:100 dilution in phosphate-buffered saline-bovine serum albumin of both anti-rabbit IgG-rhodamine isothiocyanate (Sigma) and anti-human IgG-fluorescein isothiocyanate (Sigma) and incubated for 1 h at room temperature. After this incubation, the mounted spheroplasts were washed with buffer, 1 drop of 90% buffered glycerol containing 20 mg of propyl gallate per ml was applied, and a cover slip was attached. Slides were stored at −20°C until viewing. Slides were viewed with a Zeiss standard microscope with Nomarski interference optics and fluorescein and rhodamine excitation wavelengths.

Immunoelectron microscopy. A modified procedure (detailed in reference 10) of Byers and Goetsch (6) was used for immunoelectron microscopy. On-section immune staining of ultrathin sections was performed as described previously (10, 12) except that the primary antibody used was the anti-RNA11 IgG fraction at a concentration of 2.5 μg/ml.

Sequence analysis. Sequence data were assembled, translated, and analyzed with versions 4.2 and 4.5 of the Intelligenetics GENED, SEQ, and PEP programs of the BIONET National Computer Resource for Molecular Biology. All protein sequences used in homology searches were obtained with the Intelligenetics QUEST, IFIND, and XFASTP programs with the National Institutes of Health sequence and National Biomedical Research Foundation protein data bases in BIONET.

RESULTS

Sequence of *RNA11* gene. The yeast *RNA11* gene was initially cloned by genetic complementation (31, 55). While characterizing the *SIR2* gene, Shore et al. (52) independently sequenced a 4.6-kb *Hin*dIII fragment and identified an unknown gene positioned 3′ to the *SIR2* gene. This unknown gene was shown to be essential for cell growth (52) and was later shown to be *RNA11* (R. Sternglanz, personal communication). The complete DNA sequence of the *RNA11* gene, together with the *SIR2* sequence, was deposited with the EMBL sequence library (52). In Fig. 1, we summarize the DNA sequence of the *RNA11* gene and its amino acid sequence derived from the conceptual translation. The *RNA11* gene (801 base pairs in length) codes for a protein of 266 amino acids with a calculated molecular weight of 29,924. The *RNA11* protein, which has a net charge of +7 and contains a large number of charged residues, is a highly

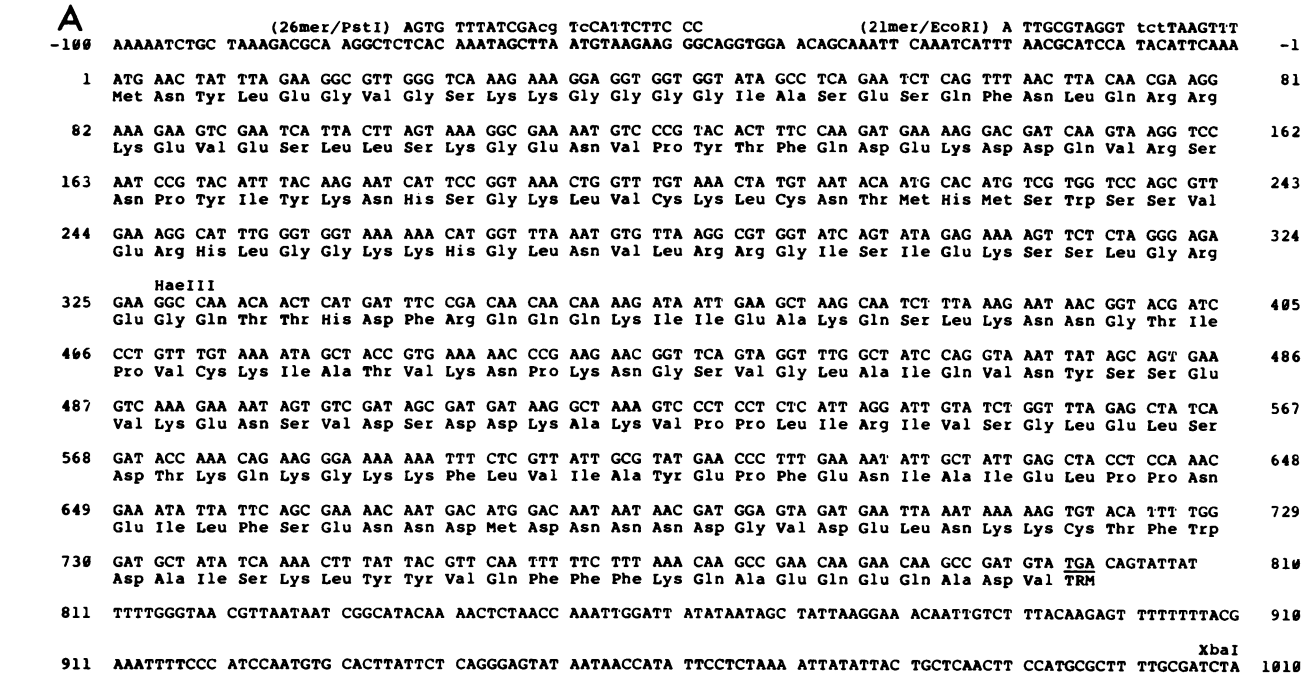

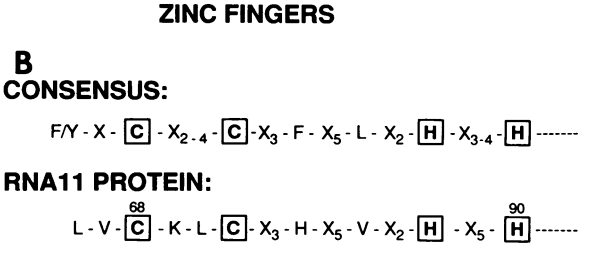

FIG. 1. Sequence of the *RNA11* gene. (A) The *RNA11* gene sequence is numbered starting from the first nucleotide of the initiation codon (ATG). The termination codon (TGA) is underlined and indicated as TRM. Upstream sequence is numbered starting as −1 for the first nucleotide adjacent to the initiation codon. 26mer/*Pst*I and 21mer/*Eco*RI are two oligonucleotides used for site-specific mutagenesis. Lowercase characters denote the mismatches. Relevant restriction sites and the conceptually translated amino acid sequence are also included. (B) The sequence of the potential zinc finger motif in the RNA11 protein is aligned with the zinc finger consensus of the C_2H_2 class (13). Highly conserved cysteine and histidine residues are boxed and their positions in the RNA11 proteins are indicated. X, Any amino acid.

hydrophilic protein as calculated by the method of Kyte and Doolittle (29). There are four methionine residues in the RNA11 protein. We compared the sequence of the RNA11 protein with the collection of protein sequences in the BIONET data bases (GenBank) and failed to find any significant homologies. However, a striking homology to the so-called zinc fingers emerged after careful inspection of the RNA11 protein sequence (Fig. 1B). The zinc finger is a structural motif that binds Zn^{2+} tightly and occurs frequently in the nucleic acid-binding proteins (reviewed in reference 13). The presence of this motif suggests that RNA11 is an RNA-binding protein.

Synthesis of RNA11 protein in vitro. To examine the role of the *RNA11* gene product during yeast mRNA splicing, we first sought to synthesize ^{35}S-labeled RNA11 protein in vitro. We started out with a plasmid, pAS1 (provided by R. Sternglanz), which contains the wild-type *RNA11* gene in a 4.6-kb *Hin*dIII fragment cloned into pBR322. A 2.7-kb *Bam*HI-*Hin*dIII fragment encompassing the entire *RNA11* gene and its flanking sequences was then subcloned into M13mp10 for site-specific mutagenesis (Fig. 2). An oligonucleotide, 26mer/*Pst*I, which hybridizes to the 5′-flanking sequence of *RNA11* at a position between −49 and −74 (Fig. 1), was utilized to introduce a *Pst*I site 63 base pairs upstream of the *RNA11* initiation codon (Fig. 2). The *Pst*I-*Xba*I fragment containing the entire *RNA11* gene with a single 5′ initiation codon was then transferred to a pSP64 transcription vector to generate plasmid pSP64-*RNA11* (Fig. 2). Transcription of the linearized pSP64-*RNA11* (by *Eco*RI or *Hae*III) plasmids in vitro with SP6 polymerase (39) yielded both the full-length and the truncated *RNA11* transcripts. These uncapped transcripts were then added to a rabbit reticulocyte lysate system for in vitro translation. The L-[^{35}S]methionine-labeled RNA11 protein synthesized in vitro had an apparent molecular weight of 32,000 (Fig. 3, lane 5). This molecular weight is in good agreement with the calculated molecular weight of 30,000. In contrast, translation of the *Hae*III-truncated *RNA11* transcript yielded a truncated RNA11 protein with an approximate size of 15 kilodaltons (kDa) (Fig. 3, lane 4). The truncated RNA11 protein is expected to be 109 amino acids long.

In vitro complementation. The activity of the in vitro-synthesized RNA11 protein in mRNA splicing was tested by an in vitro complementation assay. Normally, the heat-inactivated *rna2*, *rna5*, and *rna11* mutant extracts could complement one another, regardless of whether the extracts were mixed before or after heat inactivation (36). In contrast, when we added the RNA11 protein to the heat-

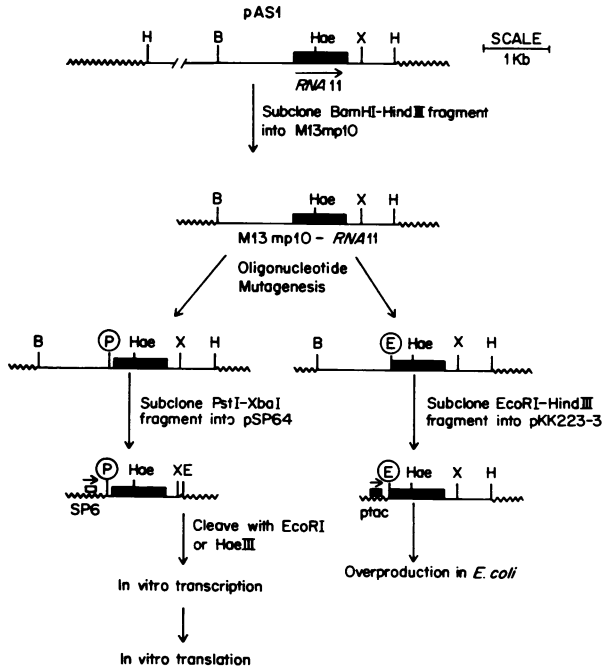

FIG. 2. Strategy to express the *RNA11* gene. The *RNA11* gene, presented as the large solid box, was originally cloned in the plasmid pAS1 and transferred to the M13mp10 vector for site-specific mutagenesis. Subsequent to mutagenesis, the *RNA11* gene was subcloned into appropriate vectors, pSP64 and pKK223-3, for in vitro transcription and in vivo overexpression, respectively. The arrow indicates the direction of *RNA11* gene transcription, and the wavy lines represent the plasmid sequences. SP6 promoter is portrayed as the small open box, and the *tax* promoter (ptac) is shown as the small solid box. B, *Bam*HI; E, *Eco*RI; Hae; *Hae*III; H, *Hin*dIII; P, *Pst*I; X, *Xba*I.

inactivated *rna11* extract (now termed the nonfunctional complementation assay), the splicing activity of the extract was not restored. We reasoned that perhaps the RNA11 protein is an integral part of a temperature-sensitive complex which, upon heat inactivation, might be permanently inactivated. The addition of the free RNA11 protein after heat inactivation would thus fail to regenerate the function of the complex (see Discussion). We therefore tested an alternative procedure (summarized in Fig. 4A) in which the heat inactivation of the *rna11* extract was performed in the presence of the RNA11 translation mix, using conditions modified from that of Lustig et al. (36). Subsequently, the ^{32}P-labeled pre-mRNA substrate (wild-type actin transcript produced in vitro) was added, and conditions were adjusted for in vitro splicing. The splicing products were then analyzed by PAGE (Fig. 4B). Under the conditions used in this assay, the full-length RNA11 protein was able to restore the splicing activity (lane 4) to a level close to that of the active *rna11* extract (no heat inactivation; lane 1), while the mock translation mix (lane 2), the translated globin (lane 3), and the translated truncated RNA11 protein (data not shown) all failed to recover the splicing activity of the *rna11* extract lost owing to heat inactivation.

Association of RNA11 protein with functional spliceosome. It has been shown that a 40S complex (spliceosome) containing pre-mRNA and intermediates of the splicing reaction will form in active yeast extracts in the presence of a functional pre-mRNA and ATP (4, 58). We wanted to investigate the fate of the RNA11 protein during spliceosome assembly. To this end, the distribution of the RNA11 protein in the course of spliceosome formation was analyzed by glycerol gradient sedimentation and SDS-PAGE (summarized in Fig. 4A). Briefly, the in vitro complementation mix was fractionated on a 50 mM KCl gradient (11 to 23% glycerol), and the spliceosome assembly was monitored by Cerenkov counting of the ^{32}P radioactivity across the gradient. Subsequently, the ^{35}S-labeled RNA11 protein as well as the ^{32}P-labeled RNAs in each fraction were precipitated with trichloroacetic acid, resolved by SDS-PAGE, and subjected to autoradiography.

A small 40S peak at fraction 11 was detected together with a larger 30S peak at fraction 15 (Fig. 5A, top). The result is consistent with the profile previously described by Lin et al. (33). This 40S complex contains pre-mRNA and intermediates of the splicing reaction, and its formation is dependent on the presence of a functional pre-mRNA and ATP (data not shown). Thus, the 40S complex is a functional spliceosome. On the other hand, the 30S complex contains exclusively the uncleaved pre-mRNA, and its formation is ATP independent and depends only on the presence of a functional pre-mRNA (data not shown; see also reference 4). The positions of the 30S and 40S peaks in the 50 mM KCl gradient were different from the results previously obtained by using 100 mM KCl gradients (4, 33, 58). It is known that the sedimentation of the splicing complexes undergoes a salt-dependent shift. At a higher salt concentration (e.g., 400 mM KCl), spliceosomes sediment more slowly than at a lower salt concentration (e.g., 50 mM KCl) in the gradient (4, 16, 17; S. Goelz and J. Abelson, unpublished data).

We then analyzed both the ^{35}S-labeled RNA11 protein and ^{32}P-labeled RNA molecules simultaneously on an SDS-polyacrylamide gel. Approximately 22 to 28% of the input RNA11 protein cosedimented with the 40S complex, and 57 to 68% cosedimented with the 30S complex (Fig. 5A, bottom). In control experiments utilizing either truncated RNA11 protein or globin for in vitro complementation, the 40S spliceosome did not form, although the 30S complex still appeared (Table 1). Neither the truncated RNA11 protein

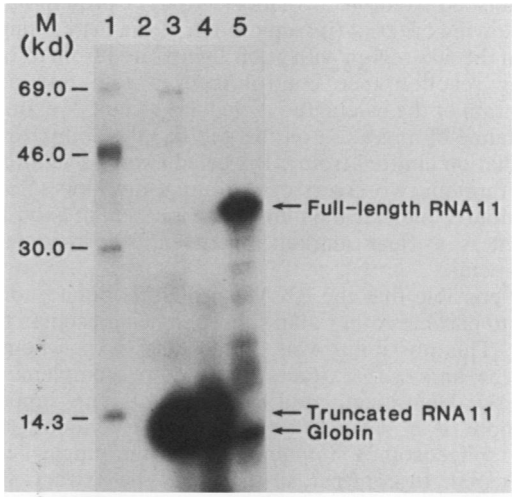

FIG. 3. In vitro translation. The in vitro-synthesized *RNA11* transcripts were translated in a rabbit reticulocyte lysate system. Lanes: 1, ^{14}C-labeled protein molecular size standards (M; in kilodaltons [kd]); 2, mock translation (minus mRNA); 3, translation of globin mRNA; 4, translation of the *Hae*III-truncated *RNA11* transcript; 5, translation of the full-length *RNA11* transcript.

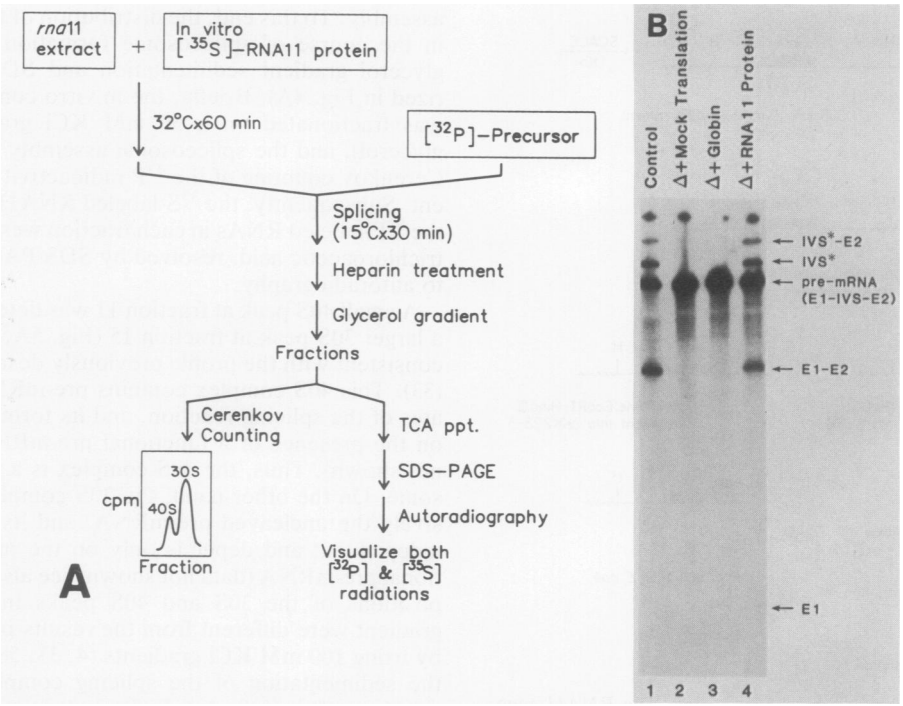

FIG. 4. In vitro complementation assay. (A) Scheme for the in vitro complementation assay. TCA, Trichloroacetic acid; ppt., precipitation. (B) Results of the complementation assays. Lanes: 1, standard splicing reaction with the *rna11* extract; 2, complementation by the mock translation mix; 3, complementation by the in vitro-translated globin product; 4, complementation by the full-length RNA11 protein. Δ, Heat inactivation; IVS*-E2, lariat intron-exon 2; IVS*, the excised lariat intron; E1-E2, the spliced message; E1, the excised exon 1.

nor the globin was associated with any complex. Instead, both proteins remained on top of the gradients (Table 1), in sharp contrast to the result with the full-length RNA11 protein.

Interestingly, the migration pattern of the RNA splicing intermediates on the SDS-polyacrylamide gel resembled that seen on a urea-polyacrylamide gel (cf. the control lane in Fig. 6A and 4B). On SDS gels, the ^{32}P-labeled exon 1 (the fastest-migrating band in the 40S region) could be clearly distinguished from the ^{35}S-labeled RNA11 protein based on the following criteria: (i) comigration of the fastest-migrating band in the 40S region with exon 1 generated from a standard splicing reaction (see control lane in Fig. 6A); (ii) the correlation of the calculated molecular weight of exon 1 with its distance of migration on the gel; (iii) the ability to detect the radiation emitted from ^{32}P-labeled exon 1 by autoradiography through two layers of opaque X-ray films (^{35}S radiation cannot penetrate the films). The location of exon 1 in the gradient is a clear marker for the spliceosome in these experiments.

It is possible that the RNA11 protein is bound nonspecifically to particles other than spliceosomes present in the 40S region. This possibility was ruled out by experiments with wild-type and *rna2* extracts for in vitro complementation (Table 1). Heat-inactivated *rna2* extracts can support the formation of a splicing-dependent 40S complex (termed rna2Δ spliceosome) containing only the uncleaved pre-mRNA (33). In contrast, in the wild-type extract, the 40S spliceosome contains the uncleaved pre-mRNA as well as the processed splicing intermediates (4). With these extracts, the input RNA11 protein did not sediment into the 40S region, but remained predominantly on top of the gradients (Fig. 5C; Table 1; see also below). Additionally, the results of the complementation experiments with either antisense or C259 mutant actin transcript also supported this argument (Table 1; described below in detail).

To ascertain that the RNA11 protein does interact with the 40S spliceosome in a highly specific fashion, we treated the complementation mix with heparin, a polyanion used to eliminate nonspecific binding of proteins to RNAs (8, 17, 26), before glycerol gradient centrifugation. This treatment resulted in the slower migration of both the 40S and 30S complexes on the gradient (Fig. 5B, top; see also reference 17), presumably owing to the removal of nonspecific, or sometimes specific (e.g., binding of U1 snRNP to the spliceosome; discussed in reference 3), binding components from these two complexes. Despite the heparin treatment, the RNA11 protein still remained bound to the 40S spliceosome (Fig. 5B, bottom). Centrifugation of the complementation mix in a high-salt (400 mM KCl) gradient gave a result similar to that of the heparin treatment, i.e., the interaction of the RNA11 protein with the now slower-migrating 40S complex still remained (Table 1). Taken together, these data indicate that the interaction between the RNA11 protein and the 40S spliceosome is specific, not fortuitous.

To show that these results are not dependent on an unknown strain effect, we repeated the in vitro complementation experiment described above (Fig. 5A) using an extract prepared from strain AJL145.9d and obtained the identical result (data not shown). Strain AJL145.9d is one of the mutant spores produced on sporulation of the diploid AJL145. This diploid was constructed by crossing the *rna11*-carrying strain, SPJ11.4, with the wild-type strain, B346B (36). The association of the RNA11 protein with the functional 40S spliceosome is therefore not likely due to genetic variations in the strain background.

Discovery of two distinct 30S complexes. Several splicing complexes have been identified in the assembly pathway of

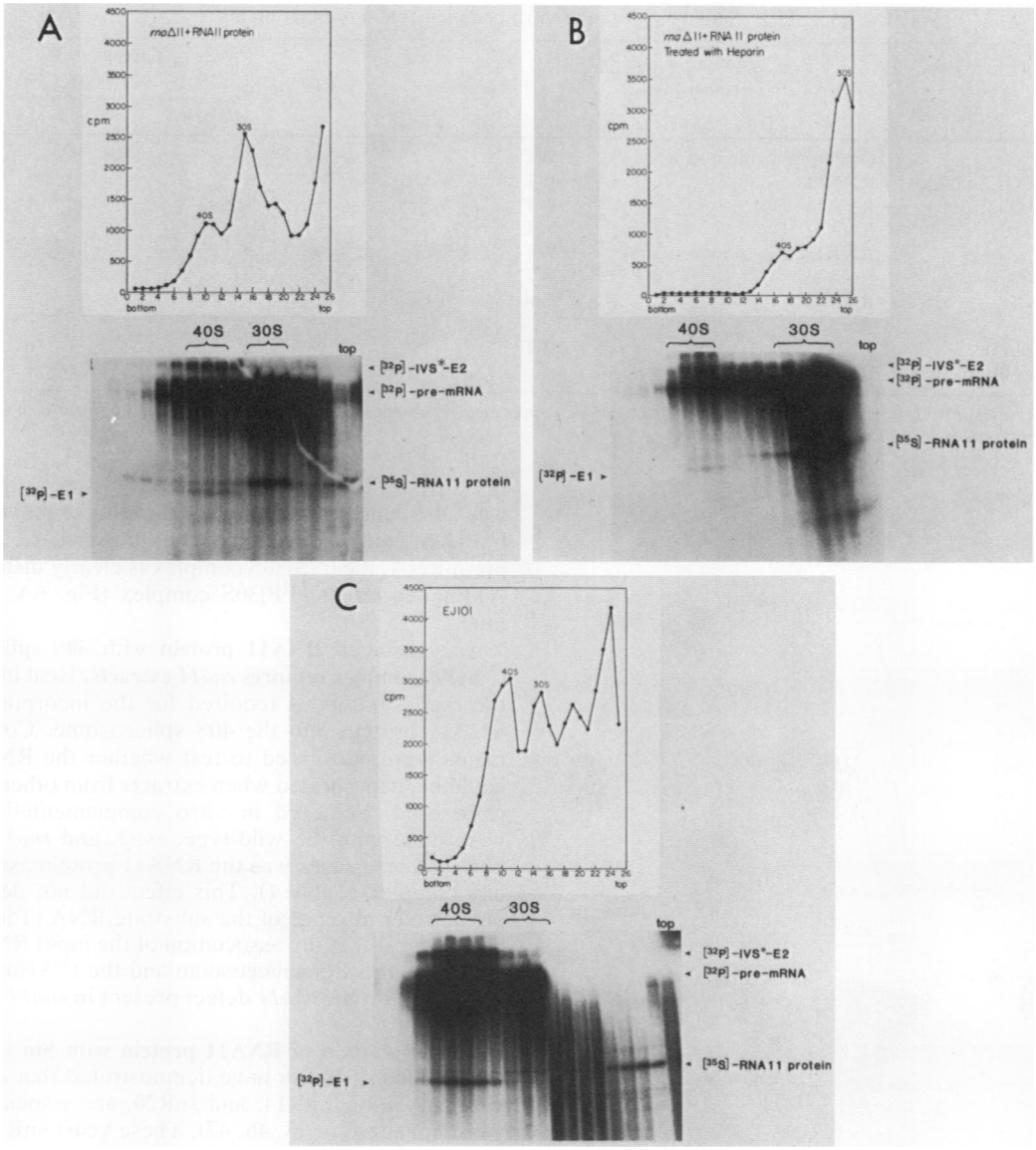

FIG. 5. Distribution of the ^{35}S-labeled RNA11 protein during in vitro complementation. Complementation mixtures were fractionated on glycerol gradients, and components in each fraction were precipitated with trichloroacetic acid and analyzed by SDS-PAGE and autoradiography. (A) Complementation with the *rna11* extract and the full-length RNA11 protein. (B) Same as panel A except treated with heparin before gradient analysis. (C) Similar to panel A except the wild-type yeast extract was used. The top panels are the Cerenkov counting profiles of the gradient fractions. The bottom panels are autoradiograms of the dried protein gels. Top and bottom, Top and bottom of the gradient; IVS*-E2 and E1, as described in the legend to Fig. 4B.

the yeast spliceosome. These complexes, resolved on either glycerol gradients or native gels, were detected by using the ^{32}P-labeled pre-mRNA (4, 8, 16, 26, 27, 46, 47, 58). A different type of 30S complex can also be defined by the presence of the ^{35}S-labeled RNA11 protein in the particle. As mentioned above, during in vitro complementation, the majority (57 to 68%) of the input ^{35}S-labeled RNA11 protein was localized in the 30S region. Thus, we have, for convenience, termed these two possible 30S complexes as the [^{32}P]30S and [^{35}S]30S complexes.

To investigate the nature of the [^{35}S]30S complex further, we performed in vitro complementation assays using two additional transcripts, the antisense actin transcript (8) and the C259 mutant transcript (58). These transcripts do not possess all the conserved sequences required for splicing and therefore cannot be assembled into the 40S spliceosome or the [^{32}P]30S complex (S.-C. Cheng and J. Abelson, unpublished data). Instead, they can only form a [^{32}P]25S complex (not precisely calibrated), presumably reflecting the yeast hnRNP particle (S.-C. Cheng and J. Abelson, unpublished data). As expected, the glycerol gradient profiles of the experiments with these two transcripts indicated that a [^{32}P]25S complex (peaked at fraction 18) was formed (Fig. 6A, top), whereas the gel analyses revealed that a distinct [^{35}S]30S complex was also assembled (peak fractions 14 and 15; Fig. 6A, bottom). This [^{35}S]30S complex contained most of the input ^{35}S-labeled RNA11 protein. Strikingly, the association of the input RNA11 protein to this [^{35}S]30S complex was completely independent of the presence of the RNA transcript, and heat inactivation of the *rna11* extract

TABLE 1. Summary of the in vitro complementation experiments[a]

Expt	Yeast extract	[35S]protein	[32P]transcript	ATP	Δ	Cerenkov 32P counting			Location of [35S]protein
						40S	30S	25S	
1	SPJ11.4	Globin or truncated RNA11	WT	+	+	−	+	−	Top
2	SPJ11.4-AJL145.9d	RNA11	WT	+	+	+	+	−	40S + 30S
3	EJ101 (WT)	RNA11	WT	+	+	+	+	−	Top
4	SS304 (*rna2*)	RNA11	WT	+	+	+	+	−	Top
5	SPJ11.4*	RNA11	WT	+	+	−	+	−	Top
6	SPJ11.4**	RNA11	WT	+	+	+	+	−	40S + 30S
7	SPJ11.4	RNA11	Antisense or C259	+	+	−	−	+	30S
8	SPJ11.4	RNA11	−	−	−	−	−	−	30S
9	RL173 (*rna5*)	RNA11	WT	+	+	−	+	−	Top
10	RL173-SS304-EJ101	RNA11	−	−	−	−	−	−	Top

[a] WT, Wild-type extract or wild-type actin transcript; Δ, heat inactivation; +, presence; −, absence; Top, top of the gradient; *, nonfunctional complementation reaction; **, sedimentation on a 400 mM KCl-glycerol gradient.

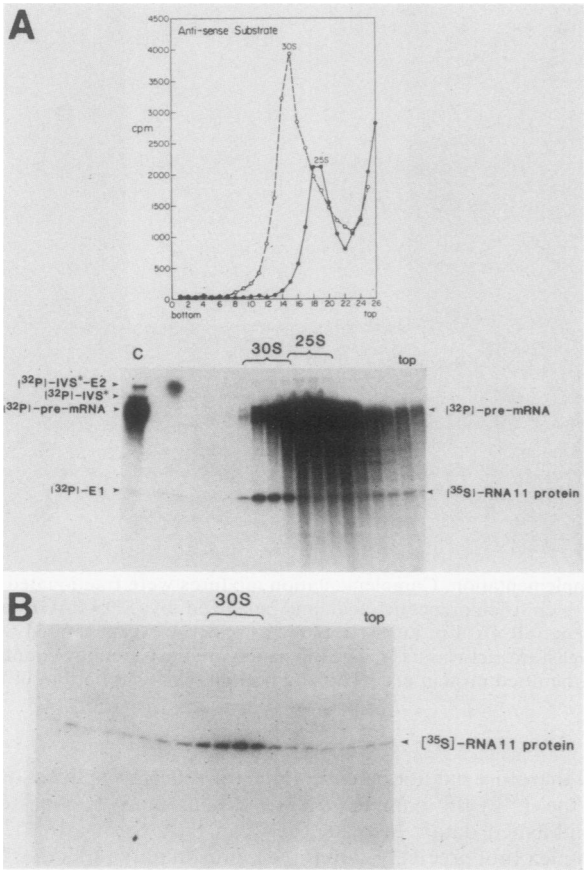

FIG. 6. Association of the RNA11 protein to the 30S complex. (A) Complementation with the *rna11* extract and the antisense transcript. The dashed line in the top panel represents the profile of the ATP-independent [32P]30S complex (see text for details) obtained from a separate experiment. Lane C, Control RNAs from a standard splicing reaction (bottom panel). IVS*-E2, IVS*, E1, As described in the legend to Fig. 4B. (B) Incubation of the RNA11 protein with the *rna11* extract in the absence of ATP, RNA transcript, and heat inactivation. The trailing of the RNA11 protein across the gradient, which can be eliminated by heparin treatment (data not shown), may represent the nonspecific association of the RNA11 protein to various cellular components in the yeast extract.

was also unnecessary (Fig. 6B). Since the formation of [32P]30S complex required the presence of a functional pre-mRNA, the [35S]30S complex is clearly distinct from the ATP-independent [32P]30S complex (Fig. 6A, top, dashed line).

Association of RNA11 protein with 40S spliceosome and [35S]30S complex requires *rna11* extracts. Heat inactivation of the *rna11* extract is required for the incorporation of the RNA11 protein into the 40S spliceosome. Control experiments were performed to test whether the RNA11 protein could be incorporated when extracts from other *rna* mutants were used. Standard in vitro complementation reactions were done with the wild-type, *rna2*, and *rna5* extracts. In none of these cases was the RNA11 protein associated with any complex (Table 1). This effect did not depend on the presence or absence of the substrate RNA (Table 1). These data suggest that the association of the input RNA11 protein with both the 40S spliceosome and the [35S]30S complex is dependent on the *rna11* defect present in *rna11* extracts (see Discussion).

Coprecipitation of RNA11 protein with Sm and m_3G epitopes. Recent studies have demonstrated that at least three snRNAs, snR7, snR14, and snR20, are associated with the yeast spliceosome (8, 46, 47). These yeast snRNAs are also immunoprecipitable by either the anti-m_3G or anti-Sm antibody (49, 50). Thus, if the RNA11 protein is indeed associated with the spliceosome or any other complexes containing the Sm or m_3G epitope during the in vitro complementation reaction, the RNA11 protein should also be immunoprecipitable by these two antibodies. This possibility was tested as follows. A complementation reaction or a nonfunctional complementation reaction (described above) was carried out and subjected to immunoprecipitation with either anti-m_3G or anti-Sm (no. 58) antibody. The immunoprecipitates were then analyzed by SDS-PAGE and autoradiography.

For the complementation reaction, approximately 6.6 and 13.8% of the input RNA11 protein could be precipitated by anti-m_3G and anti-Sm antibodies, respectively (Fig. 7, lanes 4 and 5). Conversely, when the nonfunctional complementation reaction was subjected to immunoprecipitation, only 2 to 3% of the input RNA11 protein was precipitated (Fig. 7, lanes 1 and 2). Since in such a nonfunctional complementation reaction essentially all the input 35S-labeled RNA11 protein remained free on top of the glycerol gradient (Table 1) and since the free RNA11 protein in the translation mix cannot be efficiently precipitated by either anti-m_3G or anti-Sm antibody (data not shown), this small amount (2 to

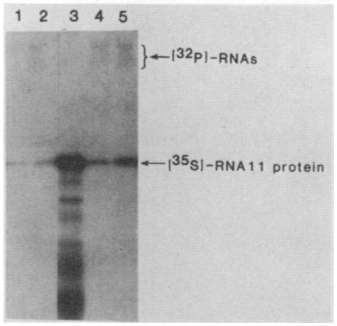

FIG. 7. Coprecipitation of the RNA11 protein and snRNP epitopes by anti-Sm and anti-m_3G antibodies. Nonfunctional complementation reactions (described in the text) were precipitated with either anti-m_3G (lane 1) or anti-Sm (no 58) (lane 2) antibody. Lanes 4 and 5 are results from a typical in vitro complementation reaction precipitated with either anti-m_3G or anti-Sm antibody, respectively. Lane 3 is the control input translated RNA11 protein without immunoprecipitation. The immunoprecipitates were resolved on an SDS-14% polyacrylamide gel. Quantitation of the radioactivity was achieved by excising the band corresponding to the ^{35}S-labeled RNA11 protein from each lane followed by liquid scintillation counting. [^{32}P]-RNAs, RNA intermediates derived from splicing of a low (1/30th of the standard)-specific-activity actin transcript.

3%) of precipitate is likely due to the background precipitation by these two antibodies. When the precipitation results for the complementation reaction were compared with those for the nonfunctional complementation reaction, there was a 3.1- and 4.5-fold increase of the precipitated RNA11 protein by anti-m_3G and anti-Sm, respectively. These data suggest that during in vitro complementation, the RNA11 protein is associated with splicing complexes, to which the m_3G and Sm antigens are also associated. Note that the ^{32}P-labeled RNA transcript, although of a lower specific activity, could also be detected as the coprecipitate (Fig. 7, lanes 4 and 5). In experiments with a transcript with a higher specific activity, coprecipitation of the RNA11 protein and the splicing intermediates (e.g., exon 1) was even more significant (data not shown). In summary, we showed that the RNA11 protein can be coprecipitated with the spliceosome or an snRNP by both anti-m_3G and anti-Sm antibodies, suggesting that the RNA11 protein is associated with splicing complexes during the in vitro complementation reaction.

Inhibition of mRNA splicing in vitro by anti-RNA11 antibody. To learn more about the role of the RNA11 protein in mRNA splicing, we raised antibodies against the RNA11 protein. Oligonucleotide mutagenesis was used to introduce an *Eco*RI site upstream of the *RNA11* gene (Fig. 1 and 2). The *RNA11* gene was then inserted into the *E. coli* expression vector pKK223-3 (5) for overexpression (Fig. 2). In this construct, the *RNA11* gene is under the control of the hybrid *trp-lac* (*tac*) promoter. *E. coli* cells containing this plasmid (pKK223-3-*RNA11*) or the parent plasmid were grown and induced with IPTG. Overproduction of the RNA11 protein was easily detected by total protein analysis on an SDS-polyacrylamide gel (Fig. 8A). A strong 32-kDa band corresponding to the size of the RNA11 protein appeared only in the pKK223-3-*RNA11*-containing cells subjected to IPTG induction (Fig. 8A, lane 4). We estimated that the overproduced protein constitutes about 5% of the total proteins in cells induced with IPTG. The overproduced protein was purified by ammonium sulfate precipitation, heparin-agarose chromatography, and preparative SDS-PAGE and used to immunize rabbits.

The specific reactivity of the antibody that was raised was ascertained by the following criteria. On immunoblots of the yeast crude extract, the antibody recognized predominantly a 32-kDa protein, close to the estimated molecular size of the RNA11 protein (Fig. 8B, lane 2). Preimmune serum failed to detect any protein in the same extract (lane 1). The antiserum was also able to detect a 32-kDa protein in the IPTG-induced *E. coli* strain carrying the plasmid pKK223-3-*RNA11* (lane 4). The 32-kDa protein was not visible in the same *E. coli* strain without IPTG induction (Fig. 8A, lane 3), nor was it detected by the antiserum (Fig. 8B, lane 3). Finally, the antibody was able to efficiently immunoprecipitate the in vitro-translated RNA11 protein (Fig. 8C, lane 8) as well as the truncated RNA11 protein (lane 6), but not the in vitro-translated globin protein (lane 4). Preimmune serum precipitated none of these in vitro-translated proteins (Fig. 8C, lanes 3, 5 and 7). Thus, we conclude that the antibody is clearly specific for the RNA11 protein.

Antibody inhibition of mRNA splicing in vitro has been used to demonstrate the critical role of snRNPs (28, 43) and hnRNPs (9, 53) involved in mRNA splicing. We applied the same approach to verify the requirement of the *RNA11* gene product for mRNA splicing.

Yeast splicing extract was preincubated with anti-RNA11, anti-m_3G, or preimmune antibody at 0°C; then splicing was allowed to take place at 23°C (Fig. 9). Addition of the preimmune antibody had no effect on splicing (lanes 1 to 3). The anti-m_3G antibody completely blocked all splicing reactions (lanes 7 and 8), even when as little as 0.5 μl was added. This result confirms the essential role of the capped snRNAs in mRNA splicing (7, 28). The addition of 3 to 7 μl of the anti-RNA11 antibody significantly inhibited splicing, although it did not block splicing completely (lanes 4 to 6). Quantitation of splicing by excision of RNA bands from the polyacrylamide gel and Cerenkov counting revealed that only 10 to 20% residual splicing remained (data not shown). Both steps of splicing were equally inhibited. Larger volumes of antibody could not be accommodated because the dilution inhibits splicing. Addition of smaller volumes of anti-RNA11 antibody caused less inhibition (data not shown). Presumably, the inability of the anti-RNA11 antibody to block splicing completely, in contrast to the results of the anti-m_3G antibody, indicates a lower titer or affinity of the antibody. Preincubation of the splicing extract with the antibody was required to achieve inhibition. Addition of the antibody at the onset of the splicing reaction did not inhibit splicing to any significant extent (data not shown), a finding in line with the work of others (9, 43, 53). Our results show that the binding of the RNA11-specific antibody to the RNA11 protein in splicing extracts prevents mRNA splicing, either by removing RNA11 protein or by altering its intrinsic activity. These results support the previous genetic observations (36) that the *RNA11* gene product is essential for mRNA splicing.

Location of RNA11 protein in periphery of the yeast nucleus. Since, as we just showed, the RNA11 protein is associated with the spliceosome, we wanted to use the anti-RNA11 antibody in immunocytological analysis to determine the cellular location of the RNA11 protein and thus the site of mRNA splicing. Because of the presumed low copy number of the RNA11 protein, the accessibility of the protein in the cells had to be optimized for the immunofluorescence procedure. The cells used for immunofluorescence were first converted to spheroplasts, mounted on glass slides, and then fixed with 3.7% formaldehyde in buffer (10).

The indirect immunofluorescence results with the wild-

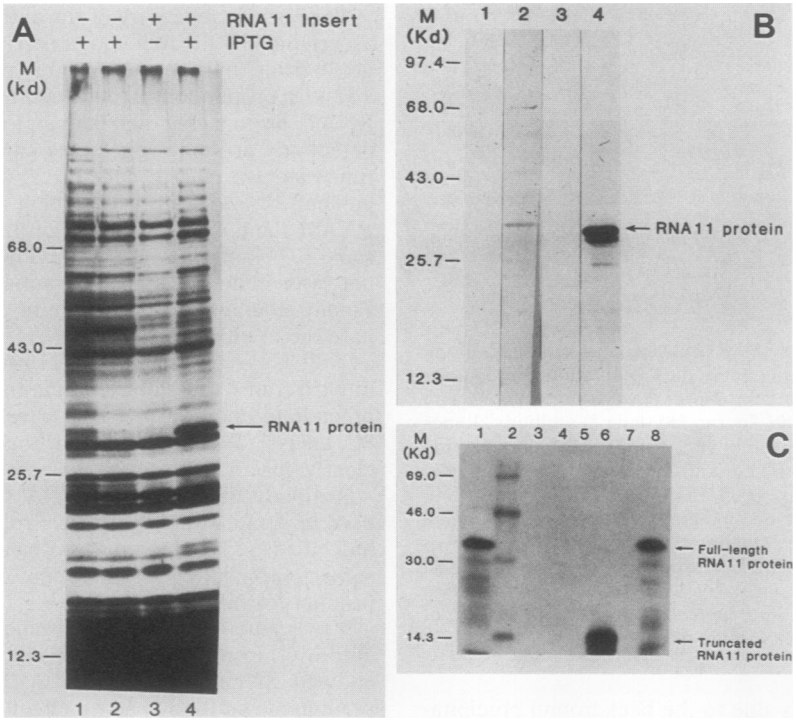

FIG. 8. Overproduction of the RNA11 protein and specific reactivity of the anti-RNA11 antibody. (A) Overproduction of the RNA11 protein in *E. coli* JM105. Total protein from cells harboring either the plasmid pKK223-3-*RNA11* (lane 3, no IPTG induction; lane 4, with IPTG induction) or the parent plasmid (pKK223-3) (lane 2) or from the plasmid-free JM105 cells (lane 1) was resolved by SDS-12% PAGE and visualized by the silver staining technique. The presence or absence of the IPTG induction and of the *RNA11* gene in the cells is indicated by + or −, respectively. M, Protein molecular size standards (kilodaltons [kd]). (B) Immunoblot analyses. Lanes 1 and 2, EJ101 yeast extract containing 50 μg of proteins was fractionated on an SDS-12% polyacrylamide gel, transferred to nitrocellulose filters, and hybridized with the preimmune (lane 1) or the anti-RNA11 immune (lane 2) serum at a dilution of 1:500. Lanes 3 and 4, *E. coli* cells harboring plasmid pKK223-3-*RNA11* were grown with (lane 4) or without (lane 3) IPTG induction and lysed in the SDS-gel loading buffer, and 10 μl of the lysate was then analyzed on an immunoblot. The dilution of the anti-RNA11 antiserum was 1:1,500. Minor bands in lane 4 may represent the breakdown products of the overproduced RNA11 protein. M, Prestained protein molecular size standards. (C) Immunoprecipitation of the in vitro-translated proteins. A 3-μl sample of the preimmune serum (lanes 3, 5, and 7) or the anti-RNA11 antiserum (lanes 4, 6, and 8) was used for precipitation. Lane 1, Input translated RNA11 protein; lane 2, ^{14}C-labeled protein molecular size standards; lanes 3 and 4, precipitation of the translated globin; lanes 5 and 6, precipitation of the translated truncated RNA11 protein; lanes 7 and 8, precipitation of the translated full-length RNA11 protein.

type yeast cells stained with an anti-RNA11 antiserum are shown in Fig. 10A. The anti-RNA11 antibody stained the nucleus but not the entire nucleus, as analyzed by Nomarski optics (see arrowheads in Fig. 10B). A preabsorption experiment (Fig. 10C) was done to show that this nuclear signal is due to the RNA11 antigen. In this experiment, 2 to 5 M equivalents of partially purified RNA11 protein were added to the anti-RNA11 antiserum dilution before the immunofluorescence staining. This treatment of the antiserum totally eliminated the nuclear signal (Fig. 10C). Thus, these data strongly suggest that the RNA11 protein is localized in a region of the yeast nucleus.

Closer examination of the nuclear location of the RNA11 protein revealed that the nuclear area stained by the anti-RNA11 antiserum, determined from 68 cells, consisted of 55% of the yeast nucleus as seen by Nomarski optics. This regional location for the RNA11 protein is most likely due to the exclusion of the RNA11 protein from the nucleolus. We tested this proposal by performing double-label immunofluorescence staining experiments using the rabbit anti-RNA11 antiserum and a human autoimmune antiserum to a nucleolar protein. This human autoimmune antiserum, referred to as fibrillarin (41), reacts with the yeast nucleolus (M. W. Clark and J. Abelson, unpublished data). The RNA11 protein appeared to be external to the nucleolus and occupied most of the nuclear area seen by Nomarski optics (Fig. 11C, arrowheads). Conversely, the fibrillarin antibody (Fig. 11B) stained only a small portion of the nucleus with a thin crescent pattern. The yeast nucleolus, unlike the nucleolus of higher organisms, has been described as a crescent attached to the nuclear envelope (24, 53). The localization for the RNA11 protein is not totally an unexpected result, since mRNA-splicing components are likely not to be required for rRNA processing.

An even more specific compartmentalization of the RNA11 protein and mRNA splicing was observed when the RNA11 protein localization was examined at a higher resolution by immunoelectron microscopy. Ultrathin sections of the Epon-embedded yeast cells were stained with the anti-RNA11 IgG or the preimmune IgG by the on-section staining technique (12). The nuclear staining pattern caused by the anti-RNA11 IgG, as visualized with a goat anti-rabbit IgG-colloidal gold conjugate, is shown in Fig. 12 A through F. Similar to the immunofluorescence mapping, the RNA11 protein, detected as 20-nm gold particles, can only be seen in a part of the yeast nucleus. To obtain quantitative evidence of the RNA11 localization, we collected data from many cell sections using the inner membrane of the nuclear envelope

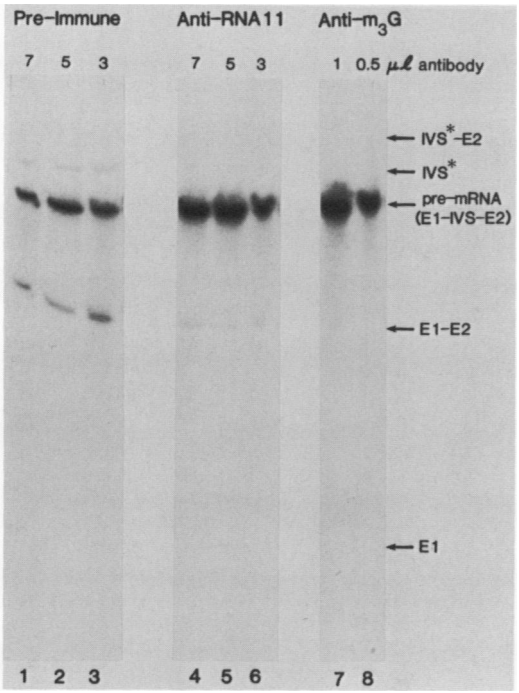

FIG. 9. Inhibition of mRNA splicing by specific antibodies. After the wild-type extract was treated with preimmune serum (7, 5, and 3 μl; lanes 1 to 3), anti-RNA11 (7, 5, and 3 μl; lanes 4 to 6), or anti-m_3G antibody (2 and 1 μl; lanes 7 and 8), a standard mRNA splicing reaction was assembled for each treated extract to assess the degree of antibody inhibition. IVS*-E2, IVS*, E1-E2, and E1, As described in the legend to Fig. 4B.

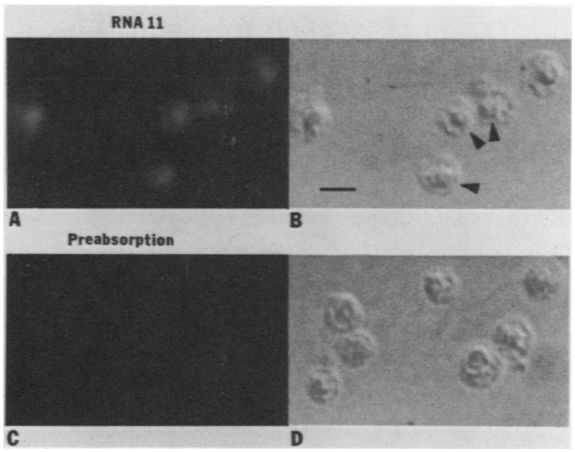

FIG. 10. Immunofluorescence of RNA11 protein and preabsorption control. (A) Formaldehyde (3.7%)-fixed spheroplasts of EJ101 cells stained with rabbit anti-RNA11 antiserum and goat anti-rabbit IgG-fluorescein isothiocyanate conjugate showing fluorescence in a region of the nucleus. (B) The same field as in panel A. The dark, convex bulge in the cell (arrowheads) is the yeast nucleus (see also reference 9). (C) Formaldehyde (3.7%)-fixed spheroplasts of EJ101 cells stained as in panel A except that 2 to 5 M equivalents of the partially purified RNA11 protein were added to the anti-RNA11 antiserum dilution. This treatment eliminates the antiserum reactivity to the RNA11 protein in the cell and removes the nuclear fluorescence. (D) Same field as in panel C. Panels A and C are viewed under fluorescein excitation wavelengths. Panels B and D are viewed by Nomarski interference optics. Bar, 5 μm.

as a point of reference and measuring the shortest distance from that point to the gold particles, both in and out of the nucleus. We then plotted these distances for anti-RNA11 IgG and preimmune IgG on the histograms shown in Fig. 12G and H, respectively. By comparing these two histograms, one can see definite staining for RNA11 in the nucleoplasm within about 300 nm from the nuclear envelope. This staining peaks around 75 to 100 nm from the nuclear envelope. The cytoplasmic staining with the anti-RNA11 antibody is probably due to the nonspecific background staining (cf. Fig. 12G and H; Table 2). We therefore conclude that the RNA11 protein is localized predominantly in the nucleoplasm at the periphery (within 300 nm) of the nuclear envelope.

DISCUSSION

In yeasts, most of the *RNA* gene products are likely to be involved in mRNA splicing in vitro (36). Their roles, however, may vary. For instance, the *RNA2* gene product is a factor extrinsic to the spliceosome required for completion of mRNA splicing, but not for the formation of the spliceosome itself (33). It is likely that many of the *RNA* gene products are integral components of the spliceosome. Our goal was to search for such a spliceosome-specific marker, which may greatly facilitate research on the spliceosome in the future. In this report, we demonstrated, using an in vitro complementation assay, that the in vitro-synthesized *RNA11* gene product is active in complementing the genetic defect of the *rna11* extract. Moreover, we found that during the in vitro complementation reaction, the RNA11 protein is associated with both the 40S spliceosome and a 30S complex. Using the anti-RNA11 antibody, we showed that the RNA11 protein is required for mRNA splicing and that the RNA11 protein is localized predominantly in the periphery of the yeast nucleus.

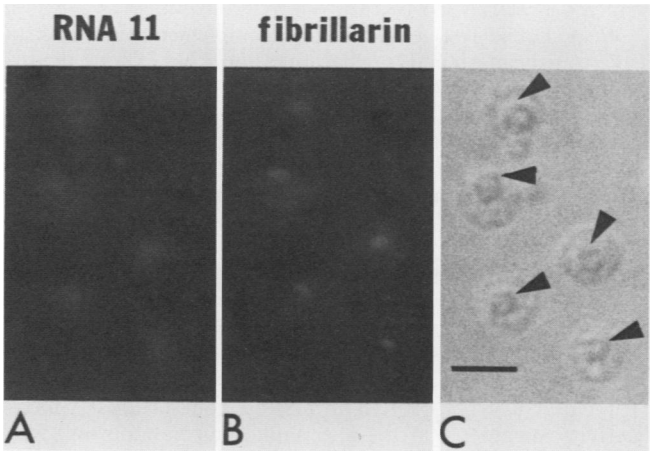

FIG. 11. Double-label immunofluorescence showing the nuclear location of the RNA111 protein relative to fibrillarin, a nucleolar protein. Formaldehyde (3.7%)-fixed spheroplasts were stained with rabbit anti-RNA11 antiserum, human anti-fibrillarin autoimmune serum (Sigma) and, as secondary antibodies, anti-rabbit IgG-rhodamine isothiocyanate conjugate and anti-human IgG-fluorescein isothiocyanate conjugate. (A) Cells viewed by rhodamine excitation wavelengths. (B) Cells viewed by fluorescein excitation wavelengths. (C) Cells viewed by Nomarski interference optics. Arrowheads point to the region of the cell nucleus which contains the antifibrillarin stain, i.e., the nucleolus. Bar, 5 μm.

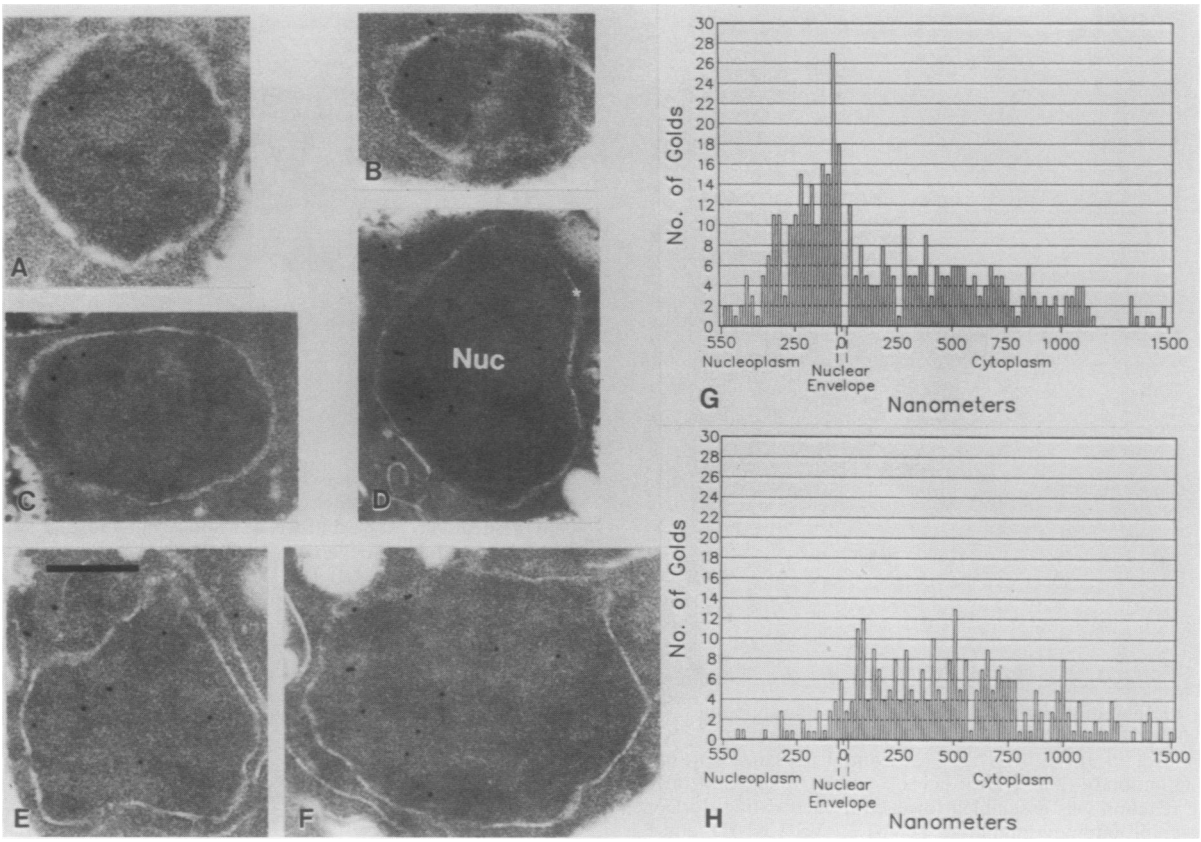

FIG. 12. Immunoelectron microscopic localization of the RNA11 protein. (A-F) Ultrathin Epon sections of EJ101 cells showing the nucleus. * in panel D indicates the lumen between the inner and outer membrane of the nuclear envelope slightly swollen by the fixation and embedding procedure. Sections are stained with rabbit anti-RNA11 IgG, and this antibody is visualized with goat anti-rabbit ItG–20-nm colloidal gold complex. Colloidal gold particles can be seen in a section of the nucleoplasm. Nuc, Nucleus. Bar, 0.5 μm. (G) Histogram of combined data from 146 cell sections stained as described for panels A through F. (H) Histogram of combined data from 155 cell sections stained as described for panels A through F except that the primary antibody was the RNA11 preimmune IgG.

***RNA11* gene product and in vitro complementation.** Successive transcription and translation of the *RNA11* gene in vitro yielded a 32-kDa RNA11 protein (Fig. 3). Under the conditions used, approximately 2.6 ng (87.5 fmol) of the RNA11 protein was synthesized per μg of the input *RNA11* transcript. Specific antibody raised against the RNA11 protein recognized predominantly a 32-kDa protein in the yeast extract and the *E. coli* RNA11-overproducer lysate (Fig. 8B), indicating the fidelity of the in vitro translation.

The in vitro-synthesized RNA11 protein could complement the defect of the *rna11* extract (Fig. 4B). The in vitro-translated globin and truncated RNA11 protein failed to do so (Fig. 4B), demonstrating a specific requirement of the RNA11 protein for complementation. The failure of the truncated RNA11 protein to complement the lost splicing activity suggests that the C-terminal half is important for a fully functional RNA11 protein. It is interesting that the complementation assay worked only when heat inactivation was performed in the presence of the RNA11 protein. The discovery that the input RNA11 protein is associated with a 30S complex in the absence of the RNA substrate (Fig. 6; Table 1) suggests a possible explanation. In the absence of the wild-type RNA11 protein, heat inactivation may irreversibly destroy this endogenous 30S complex containing the mutant RNA11 protein. In the presence of the wild-type RNA11 protein, exchange between the mutant RNA11 protein and its wild-type counterpart could perhaps stabilize or preserve the function of this complex. This proposal can be supported by previous data (36, 37), which have demonstrated a free exchange of the components involved in spliceosome assembly. Wild-type RNA11 protein in the 30S complex may not exchange with the exogenously added wild-type RNA11 protein owing to the intrinsic stability of the 30S complex. Indeed, in experiments with wild-type, *rna2*, or *rna5* extract, the input RNA11 protein did not associate with any complex (Table 1).

TABLE 2. RNA11 immunoelectron microscope data quantitation

Area of cell	Anti-RNA11 golds (%)	Preimmune golds (%)
Nucleoplasm	183 (44)	23 (8)
Nuclear envelope	18 (4)	9 (3)
Cytoplasm	217 (52)	260 (89)

Association of RNA11 protein with 40S spliceosome. Two lines of evidence suggest that the RNA11 protein is associated with the 40S spliceosome during in vitro complementation. First, upon glycerol gradient sedimentation, a significant fraction of the input RNA11 protein comigrated with the 40S spliceosome (Fig. 5A) and remained so despite stringent treatments with either heparin or high salt (Fig. 5B; Table 1). Second, anti-Sm and anti-m_3G antibodies were able to

coprecipitate the RNA11 protein and the RNA splicing intermediates (Fig. 7). Recent immunoelectron microscopy studies with anti-RNA11 IgG to label the purified spliceosomes also suggest that RNA11 protein is present in the spliceosome (M. W. Clark et al., manuscript in preparation).

One can calculate the stoichiometry between the RNA11 protein and the spliceosome by assuming that there is one exon 1 per spliceosome. The calculated result is 0.3 to 0.4 (RNA11 protein/exon 1), but the interpretation of this number is complicated by the finding that several spliceosome intermediates are involved in the mRNA splicing pathway (8, 27, 47). Thus, the spliceosome as originally defined (4) is in fact a mixture of all these complexes, so there are likely to be 40S complexes which do not contain RNA splicing intermediates.

Nature of 30S complexes. During the in vitro complementation reaction, the RNA11 protein was also associated with a 30S particle (Fig. 5A and B). Two 30S complexes can be separately defined, namely, the [^{32}P]30S and the [^{35}S]30S complexes. The ATP-independent [^{35}S]30S complex was detected only when the *rna11* extract was used for the complementation assay, and its formation was independent of the exogenously added RNA substrate (Fig. 6B; Table 1). This is in contrast to the ATP-independent [^{32}P]30S complex, which forms in active yeast extracts and requires the presence of a functional pre-mRNA (4, 58). It is interesting to note that Frendewey and Keller (15) have reported a 35S preslicing complex, likely to be the [^{32}P]30S counterpart in the HeLa cell system, formed in the absence of ATP. The [^{35}S]30S complex is also distinct from the 25S complex, which formed on RNA substrates lacking all the required splicing signals (Fig. 6A). The 25S complex may represent the yeast hnRNP particles, for it forms on many RNAs lacking the splicing signals (S.-C. Cheng and J. Abelson, unpublished data).

What is the nature of the [^{35}S]30S complex? One attractive possibility is that it represents an snRNP or a complex of several snRNPs in the yeast extract. Konarska and Sharp (27) have recently reported that a 25S multi-snRNP particle containing U4/6 and U5 snRNPs is preformed in the HeLa nuclear extract and proposed that this multi-snRNP complex interacts with the U2-bound pre-mRNA to form the mature spliceosome. Interestingly, Cheng and Abelson (8) have also identified such a multi-snRNP in the yeast extract containing snRNAs (snR14, snR6, and snR7) homologous to the mammalian U4, U6, and U5, respectively. Unfortunately, the sedimentation coefficient of the yeast multi-snRNP is currently unknown. Most recently, Lossky et al. (35) have demonstrated, using anti-RNA8 antibodies, that the RNA8 protein is in stable association with snR7 and undergoes an additional ATP-dependent association with snR14 and snR6. These data are in good agreement with the observations described above, raising the possibility that the RNA11 protein is also an snRNP protein. Our preliminary studies with the RNA11-specific antibody failed to detect any snRNA specifically bound to the RNA11 protein. Perhaps RNA11 protein is not easily accessible to the antibody, as suggested by our antibody inhibition experiments (Fig. 9), or perhaps it is simply loosely bound to an snRNP. It is also possible that the [^{35}S]30S complex is a large snRNP consisting of a single snRNA of extraordinary length, such as snR20 (1,175 nucleotides) or snR19 (569 nucleotides). Future work is required to explore all these possibilities. The relationship between [^{35}S]30S and [^{32}P]30S complexes, if any, also remains an open question.

Inhibition of splicing by anti-RNA11 antibody. A functional *RNA11* gene is essential for mRNA splicing in vitro (36) and for cellular viability in vivo (52). The former was confirmed by the antibody inhibition experiment, in which the splicing reaction was greatly diminished by preincubating the wild-type yeast extract with the anti-RNA11 antibody (Fig. 9). Unlike the complete inhibition of the splicing reaction by anti-m_3G antibody, anti-RNA11 antibody only partially diminished the splicing activity. This may be attributed to a lower titer or affinity of the anti-RNA11 antibody compared with that of the anti-m_3G antibody, or it may be due to only the partial accessibility of the RNA11 antigen in the yeast extract. Anti-RNA11 antibody inhibited both steps of splicing equally well, indicating that it either acts at the step before the first cleavage reaction, as previously suggested by Lin et al. (33), or interferes equally at both cleavage and ligation reactions.

Subnuclear location of RNA11 protein. A previous immunofluorescence study has placed the overproduced RNA2 and RNA3 proteins in the yeast nucleus (32). Our immunofluorescence-determined nuclear location for wild-type levels of the RNA11 protein agrees with this study. Our studies also demonstrated that at least one of the *RNA* gene products (i.e., the RNA11 protein) does not reside in the yeast nucleolus. About one-third of the yeast nuclear volume is directed toward rRNA synthesis and preribosome assembly (54). The mRNA-splicing components appear not to have access to this area of the nucleus. This compartmentalization of function in the yeast nucleus seems to extend to even finer detail.

We showed that the RNA11 protein is located in the periphery of the nucleus, within a region 250 to 300 nm in from the nuclear envelope. The peak of the RNA11 protein location is about 75 to 100 nm in from the nuclear envelope. Other mRNA-splicing components show this same nuclear location. For instance, the anti-Sm (no. 58) antiserum was used in immunoelectron microscopy to localize the yeast Sm antigens, and its localization pattern appears to be similar to that of the RNA11 protein (M. W. Clark and J. Abelson, unpublished data). The compartmentalization of mRNA-splicing components that we observed in yeast cells has also been found in higher eucaryotes. Fakan and co-workers (14) have examined the distribution of hnRNPs and snRNPs by immunoelectron microscopy. By immunofluorescence microscopy, hnRNPs and snRNPs show both a distinct punctate and a diffuse nuclear staining pattern; in their study, Fakan and co-workers (14) present electron micrographs which reveal that the staining for both of these particles predominates in the periphery of the rat liver nucleus. These data, taken together, indicate that the mRNA-splicing components are not only sequestered into a macromolecular complex, the spliceosome, they are also located in a specific nuclear subcompartment, the nuclear periphery. One explanation for this subnuclear localization of mRNA splicing is that mRNA transcription is also occurring in the nuclear periphery. The mRNA-splicing components thus become localized by binding to the nascent precursor mRNAs.

Recent experiments to map the site of mRNA transcription place transcription components in the nuclear periphery. The yeast heat shock transcription factor, which binds to the promoter regions of the yeast heat shock genes (59), has been mapped by immunofluorescence and immunoelectron microscopy to the same sites as the RNA11 and Sm proteins (M. W. Clark and J. Abelson, unpublished data). Also by immunoelectron microscopy, Clark and Hamkalo (11) have localized RNA polymerase II in the periphery of the mouse cell nucleus. This phenomenon of compartmen-

talization of nuclear mRNA function seems to extend from yeasts to mammals and indicates its importance in proper nuclear function. The existence of a specific mechanism responsible for this nuclear organization may also be implied from these data. The tissue-specific ordering of the chromosomes reported in *Drosophila* larva nuclei (22, 23), Purkinje cell nuclei (38), and plant cell nuclei (21) might account for the observed compartmentalization of RNA-processing functions. In such a model of nuclear organization, the chromosomes would be arranged so that the sites of transcription are at the nuclear periphery where the RNA-processing enzymes are concentrated. Experiments to investigate the placement of the chromosomes in the yeast interphase nucleus are currently under way (M. W. Clark and J. Abelson, unpublished data).

ACKNOWLEDGMENTS

We thank R. Lührmann and S. Hoch for providing anti-m_3G and anti-Sm (no. 58) antisera, respectively, and R. Sternglanz for supplying the cloned *RNA11* gene. We also thank E. Grayhack, S. Goelz, S.-C. Cheng, R.-J. Lin, J. Dahlberg, and S. Westaway for their stimulating discussions and technical advice. The critical reading of the manuscript by U. Vijayraghavan and K. Tanner is also greatly appreciated. We thank D. McPheeters for pointing out the potential zinc finger motif in the RNA11 protein.

Computer resources were provided by BIONET National Computer Resource for Molecular Biology, whose funding is provided by the Biomedical Research Technology Program, Division of Research Resources, National Institutes of Health (grant 1-U41RR-01685-05). M.E.C. is supported by a postdoctoral fellowship (S-12-86) from the American Cancer Society. This work was supported entirely by a Public Health Service grant awarded to J.A. from the National Institutes of Health.

LITERATURE CITED

1. **Adams, A. E. M., and J. R. Pringle.** 1984. Relationship of actin and tubulin distribution to bud growth in wild-type and morphogenetic-mutant *Saccharomyces cerevisiae*. J. Cell Biol. **98:** 934–945.
2. **Ares, M., Jr.** 1986. U2 RNA from yeast is unexpectedly large and contains homology to vertebrate U4, U5, and U6 small nuclear RNAs. Cell **47:**49–59.
3. **Bindereif, A., and M. R. Green.** 1987. An ordered pathway of snRNP binding during mammalian pre-mRNA splicing complex assembly. EMBO J. **6:**2415–2424.
4. **Brody, E., and J. Abelson.** 1985. The "spliceosome": yeast pre-messenger RNA associates with a 40S complex in a splicing-dependent reaction. Science **228:**963–967.
5. **Brosius, J., and A. Holy.** 1984. Regulation of ribosomal RNA promoters with a synthetic *lac* operator. Proc. Natl. Acad. Sci. USA **81:**6929–6933.
6. **Byers, B., and L. Goetsch.** 1975. The behavior of spindles and spindle plaques in the cell cycle and conjugation of *Saccharomyces cerevisiae*. J. Bacteriol. **124:**511–523.
7. **Cheng, S.-C., and J. Abelson.** 1986. Fractionation and characterization of a yeast mRNA splicing extract. Proc. Natl. Acad. Sci. USA **83:**2387–2391.
8. **Cheng, S.-C., and J. Abelson.** 1987. Spliceosome assembly in yeast. Genes Dev. **1:**1014–1027.
9. **Choi, Y. D., P. J. Grabowski, P. A. Sharp, and G. Dreyfuss.** 1986. Heterogeneous nuclear ribonucleoproteins: role in RNA splicing. Science **231:**1534–1539.
10. **Clark, M. W., and J. Abelson.** 1987. The subnuclear localization of tRNA ligase in yeast. J. Cell Biol. **105:**1515–1526.
11. **Clark, R. F., and B. A. Hamkalo.** 1987. Localization of nuclear proteins by immunogold staining and electron microscopy. J. Cell Biol. **105:**71a.
12. **Demay, J.** 1983. A critical review of light and electron microscopic immunocytochemical techniques used in neurobiology. J. Neurosci. Methods **7:**1–18.
13. **Evans, R. M., and S. M. Hollenberg.** 1988. Zinc fingers: gilt by association. Cell **52:**1–3.
14. **Fakan, S., G. Leser, and T. E. Martin.** 1984. Ultrastructural distribution of nuclear ribonucleoproteins as visualized by immunocytochemistry on thin sections. J. Cell Biol. **98:**358–363.
15. **Frendewey, D., and W. Keller.** 1985. Stepwise assembly of a pre-mRNA splicing complex requires U-snRNAs and specific intron sequences. Cell **42:**355–367.
16. **Grabowski, P. J., S. R. Seiler, and P. A. Sharp.** 1985. A multicomponent complex is involved in the splicing of messenger RNA precursors. Cell **42:**345–353.
17. **Grabowski, P. J., and P. A. Sharp.** 1986. Affinity chromatography of splicing complexes: U2, U5 and U4/U6 small nuclear ribonucleoprotein particles in the spliceosome. Science **233:** 1294–1299.
18. **Guthrie, C.** 1986. Finding functions for small nuclear RNAs in yeast. Trends Biochem. Sci. **11:**430–434.
19. **Guthrie, C., N. Riedel, R. Parker, H. Swerdlow, and B. Patterson.** 1986. Genetic analyses of snRNAs and RNA processing in yeast. UCLA Symp. Mol. Cell. Biol. New Series **33:**301–321.
20. **Hartwell, H. L.** 1967. Macromolecule synthesis in temperature-sensitive mutants of yeast. J. Bacteriol. **93:**1662–1670.
21. **Heslop-Harrison, J. S., and M. D. Bennett.** 1984. Chromosome order-possible implications for development. J. Embryol. Exp. Morphol. Suppl. **83:**51–73.
22. **Hochstrasser, M., and J. W. Sedat.** 1987. Three-dimensional organization of *Drosophila melanogaster* interphase nuclei. I. Tissue-specific aspects of polytene nuclear architecture. J. Cell Biol. **104:**1455–1470.
23. **Hochstrasser, M., and J. W. Sedat.** 1987. Three-dimensional organization of *Drosophila melanogaster* interphase nuclei. II. Chromosome spatial organization and gene regulation. J. Cell Biol. **104:**1471–1483.
24. **Jong, A. Y.-S., M. W. Clark, M. Gilbert, A. Oehm, and J. L. Campbell.** 1987. *Saccharomyces cerevisiae* SSB1 protein and its relationship to nucleolar RNA-binding proteins. Mol. Cell. Biol. **7:**2947–2955.
25. **Kilmartin, J. V., and A. E. M. Adams.** 1984. Structural rearrangements of tubulin and actin during the cell cycle of yeast *Saccharomyces cerevisiae*. J. Cell Biol. **98:**922–933.
26. **Konarska, M. M., and P. A. Sharp.** 1986. Electrophoretic separation of complexes involved in the splicing of precursors to mRNAs. Cell **46:**845–855.
27. **Konarska, M. M., and P. A. Sharp.** 1987. Interactions between small nuclear ribonucleoprotein particles in formation of spliceosomes. Cell **49:**763–774.
28. **Kramer, A., W. Keller, B. Appel, and R. Lührmann.** 1984. The 5′ terminus of the RNA moiety of U1 small nuclear ribonucleoprotein particles is required for the splicing of messenger RNA precursors. Cell **38:**299–307.
29. **Kyte, J., and R. F. Doolittle.** 1982. A simple method for displaying the hydropathic character of a protein. J. Mol. Biol. **157:**105–132.
30. **Laemmli, U. K.** 1970. Cleavage of structural proteins during assembly of the head of bacteriophage T4. Nature (London) **227:**680–685.
31. **Last, R. L., J. B. Stavenhagen, and J. L. Woolford.** 1984. Isolation and characterization of the *RNA2*, *RNA3*, and *RNA11* genes of *Saccharomyces cerevisiae*. Mol. Cell. Biol. **4:**2396–2405.
32. **Last, R. L., and J. L. Woolford.** 1986. Identification and nuclear localization of yeast pre-messenger RNA processing components: RNA2 and RNA3 proteins. J. Cell Biol. **103:**2103–2112.
33. **Lin, R.-J., A. J. Lustig, and J. Abelson.** 1987. Splicing of yeast nuclear pre-mRNA in vitro requires a functional 40S spliceosome and several extrinsic factors. Genes Dev. **1:**7–18.
34. **Lin, R.-J., A. J. Newman, S.-C. Cheng, and J. Abelson.** 1985. Yeast mRNA splicing in vitro. J. Biol. Chem. **260:**14780–14792.
35. **Lossky, M., G. J. Anderson, S. P. Jackson, and J. Beggs.** 1988. Identification of a yeast snRNP protein and detection of snRNP-snRNP interactions. Cell **51:**1019–1026.
36. **Lustig, A. J., R.-J. Lin, and J. Abelson.** 1986. The yeast *RNA* gene products are essential for mRNA splicing in vitro. Cell

47:953–963.
37. **Maniatis, T., and R. Reed.** 1987. The role of small nuclear ribonucleoprotein particles in pre-mRNA splicing. Nature (London) **325**:673–678.
38. **Manuelidis, L.** 1984. Different central nervous system cell types display distinct and nonrandom arrangements of satellite DNA sequences. Proc. Natl. Acad. Sci. USA **81**:3122–3127.
39. **Melton, D. A., P. A. Krieg, M. R. Rebagliati, T. Maniatis, K. Zinn, and M. R. Green.** 1984. Efficient in vitro synthesis of biologically active RNA and RNA hybridization probes from plasmids containing a bacteriophage SP6 promoter. Nucleic Acids Res. **12**:459–472.
40. **Newman, A. J., R.-J. Lin, S.-C. Cheng, and J. Abelson.** 1985. Molecular consequences of specific intron mutations on yeast mRNA splicing in vivo and in vitro. Cell **42**:335–344.
41. **Ochs, R. L., M. A. Lischwe, W. H. Spohn, and H. Busch.** 1985. Fibrillarin: a new protein of the nucleolus identified by autoimmune sera. Biol. Cell **154**:123–134.
42. **Padgett, R. A., P. J. Grabowski, M. M. Kornaska, S. Seiler, and P. A. Sharp.** 1986. Splicing of messenger RNA precursors. Annu. Rev. Biochem. **55**:1119–1150.
43. **Padgett, R. A., S. M. Mount, J. A. Steitz, and P. A. Sharp.** 1983. Splicing of messenger RNA precursors is inhibited by antisera to small nuclear ribonucleoprotein. Cell **35**:101–107.
44. **Patterson, B., and C. Guthrie.** 1987. An essential yeast snRNA with a U5-like domain is required for splicing in vivo. Cell **49**: 613–624.
45. **Phizicky, E. M., R. C. Schwartz, and J. Abelson.** 1986. *Saccharomyces cerevisiae* tRNA ligase. J. Biol. Chem. **261**:2978–2986.
46. **Pikielny, C. W., and M. Rosbash.** 1986. Specific small nuclear RNAs are associated with yeast spliceosome. Cell **45**:869–877.
47. **Pikielny, C. W., B. C. Rymond, and M. Rosbash.** 1986. Electrophoresis of ribonucleoproteins reveals an ordered assembly pathway of yeast splicing complexes. Nature (London) **324**: 341–345.
48. **Reddy, R., and H. Busch.** 1983. Small nuclear RNAs and RNA processing. Prog. Nucleic Acid Res. Mol. Biol. **30**:127–162.
49. **Riedel, N., J. A. Wise, H. Swerdlow, A. Mak, and C. Guthrie.** 1986. Small nuclear RNAs from *Saccharomyces cerevisiae*: unexpected diversity in abundance, size, and molecular complexity. Proc. Natl. Acad. Sci. USA **83**:8097–8101.
50. **Riedel, N., S. Wolin, and C. Guthrie.** 1987. A subset of yeast snRNA's contains functional binding sites for the highly conserved Sm antigen. Science **235**:328–331.
51. **Rosbash, M., P. K. W. Harris, J. L. Woolford, and J. L. Teem.** 1981. The effect of temperature-sensitive *rna* mutants of the transcription products from cloned ribosomal protein genes of yeast. Cell **24**:679–686.
52. **Shore, D., M. Squire, and K. A. Nasmyth.** 1984. Characterization of two genes required for the position-effect control of yeast mating-type genes. EMBO J. **3**:2817–2823.
53. **Sierakowska, H., W. Szer, P. J. Furdon, and R. Kole.** 1986. Antibodies to hnRNP core proteins inhibit in vitro splicing of human β-globin pre-mRNA. Nucleic Acids Res. **14**:5241–5254.
54. **Sillevis-Smitt, W. W., J. M. Vlak, I. Molenaar, and T. H. Rozijn.** 1973. Nucleolar function of the dense crescent in the yeast nucleus. Exp. Cell Res. **80**:313–321.
55. **Soltyk, A., M. Tropak, and J. D. Friesen.** 1984. Isolation and characterization of the *RNA2*$^+$, *RNA4*$^+$, and *RNA11*$^+$ genes of *Saccharomyces cerevisiae*. J. Bacteriol. **160**:1093–1100.
56. **Steiz, J. A., S. L. Wolin, J. Rinke, I. Pettersson, S. M. Mount, E. A. Lerner, M. Hinterberger, and E. Gottlieb.** 1983. Small ribonucleoproteins from eukaryotes: structures and roles in RNA biogenesis. Cold Spring Harbor Symp. Quant. Biol. **47**: 893–900.
57. **Towbin, H., T. Staehelin, and J. Gordon.** 1979. Electrophoretic transfer of proteins from polyacrylamide gels to nitrocellulose sheets: procedure and some applications. Proc. Natl. Acad. Sci. USA **79**:5188–5189.
58. **Vijayraghavan, U., R. Parker, J. Tamm, Y. Iimura, J. Rosi, J. Abelson, and C. Guthrie.** 1986. Mutations in conserved intron sequences affect multiple steps in the yeast splicing pathway, particularly assembly of the spliceosome. EMBO J. **5**: 1683–1695.
59. **Wiederrecht, G., D. J. Shuey, W. A. Kibbe, and C. S. Parker.** 1987. The *Saccharomyces* and *Drosophila* heat shock transcription factors are identical in size and DNA binding properties. Cell **48**:507–515.
60. **Wise, J. A., D. Tollervey, D. Maloney, H. Swerdlow, E. J. Dunn, and C. Guthrie.** 1983. Yeast contains small nuclear RNAs encoded by single copy genes. Cell **35**:743–751.
61. **Wolin, S. L., and J. A. Steitz.** 1984. The Ro small cytoplasmic ribonucleoproteins: identification of the antigenic protein and its binding site on the Ro RNAs. Proc. Natl. Acad. Sci. USA **81**: 1996–2000.
62. **Wray, W., T. Boulikas, V. P. Wray, and R. Hancock.** 1981. Silver staining of proteins in polyacrylamide gels. Anal. Biochem. **118**:197–203.